Distributed Circular Formation Control of Nonholonomic Vehicles Without Direct Distance Measurements

Xiao Yu, *Member, IEEE*, Lu Liu, *Senior Member, IEEE*, and Gang Feng, *Fellow, IEEE*

***Abstract*—This note presents a static distributed formation control law for nonholonomic vehicles subject to velocity constraints, such that the controlled vehicles travel along a common circle with the given center and radius, while maintaining a desired spaced formation. The center is assumed to be known to only some vehicles. The proposed controller does not require any communication, and only uses local measurements based on a sensor graph of which the topology is modeled by a directed graph satisfying a certain acyclic condition. Moreover, direct distance measurements are not needed. Finally, the simulation results of an example verify effectiveness of the proposed controller.**

***Index Terms*—Circular formation, distributed control, local measurements, nonholonomic vehicles, velocity constraints.**

I. Introduction

Formation and coordination control of multi-agent systems have attracted tremendous research interests since the early years of this century [1–3]. Due to the potential applications to sensor networks, source seeking exploration, and robotic surveillance, circular formation of nonholonomic vehicles has become a hot topic of interest. The objective of circular formation control is to make multiple vehicles orbit around a center and maintain a spaced formation. Circular formation control can be divided into two categories. The first category considers an unspecified center [4–12] and is also referred to as collective circular motion. The other one considers a given center [6, 13–20] and is often referred to as target-enclosing or circumnavigation.

For the first category, the center is generally dependent on initial positions of vehicles. In [4, 5], vehicles in cyclic pursuit was studied. In [6, 7], gradient control laws based on potential functions were developed for vehicles under complete and balanced communication graphs respectively. In [12], vehicles with nonidentical constant velocities were further considered. In [9, 10], sensor ranges of vehicles were taken into account and a jointly connected condition on proximity graph was presented. In [11], dynamic unicycles under a directed sensor graph were considered and the local stability of the closed-loop system was established.

Manuscript received April 24, 2017; revised October 1, 2017; accepted November 13, 2017. Date of publication January 5, 2018. This work was supported by the Research Grants Council of the Hong Kong Special Administrative Region of China under Project CityU/11213415. Recommended by Associate Editor M. Cao. (*Corresponding author: Lu Liu*)

X. Yu is now with the Department of Automation, Shanghai Jiao Tong University, Shanghai 200240, China, and was with the Department of Mechanical and Biomedical Engineering, City University of Hong Kong, Kowloon, Hong Kong (e-mail: xiaoyu4-c@my.cityu.edu.hk).

L. Liu and G. Feng are with the Department of Mechanical and Biomedical Engineering, City University of Hong Kong, Kowloon, Hong Kong SAR, China. (e-mail: luliu45@cityu.edu.hk, megfeng@cityu.edu.hk).

Since the center can represent a target or a beacon, many works focused on the second category. It was assumed in most existing works that the center is known to all vehicles. In [6], a gradient control law drove vehicles around a beacon with different spacing arrangements. In [13], limited visibility of onboard sensors was considered, but the objective for spaced formation was not included. In [14], spaced formation along the circle was addressed based on rigidity of the sensor graph. Several works studied evenly-spaced formation of ring-coupled vehicles. In particular, a hybrid control law based on local measurements was developed in [15]. In [18], it was shown that the controlled vehicles converge to circumnavigation around a center with nonidentical given radii. For the case where the center is known to only one vehicle, a distributed control law using both local measurements and communication was proposed in [17] for cycle vehicle networks, which was extended to general directed networks in [19]. In [20], circumnavigation with nonidentical radii was investigated.

All aforementioned works in both categories assumed relative position or distance measurements are available, which renders their practical applications limited. In some scenarios, distances cannot be accurately measured or even worse cannot be obtained at all, for instance, mobile wheeled robots with only cameras, or unmanned aerial vehicles without lidars. To address this restriction, several attempts were made to formation control of holonomic agents [21–23]. For nonholonomic vehicles, triangular formation control [24, 25], leader-following tracking control [26, 27], and balanced circular formation control for vehicle networks modeled by a complete graph or a cycle [8] were studied. Recently in [16], controllers using bearing angle measurements were developed such that multiple vehicles can enclose a target (center) with an evenly-spaced formation. However, the target was assumed to be known to all vehicles.

In this note, a circular formation control problem similar to [6, 14–17] is considered. The center of the circular formation is given and known to only some vehicles. The sensor graph is modeled by a directed graph satisfying a certain acyclic condition. A distributed controller without direct distance measurements is proposed, such that circular formation with a given center and any desired spacing can be achieved.

The main contributions of this work can be summarized into four aspects. First, compared with [6, 14–16], the proposed control law is distributed in the sense that the center of circular formation is known to only some vehicles. Second, compared with [6, 14, 15, 17], the proposed controller does not need the relative position or distance measurements, and compared with [17], the communication and the memory are not required, which makes its implementation easier in practice. Third,

compared with [8, 15–17], the global convergence to any desired spaced formation instead of only an evenly-spaced one can be achieved. Last but not least, compared with [6, 15, 16], velocity constraints of each vehicle can be satisfied.

The rest of this note is organized as follows. In Section II, we give the problem formulation and review three technical lemmas. In Section III, a distributed controller is proposed and the stability of the closed-loop system is established. In Section IV, the simulation results of an example are presented, and in Section V, the conclusion is drawn.

Notations: The norm $\|\boldsymbol{x}\|$ of a vector $\boldsymbol{x}=\text{col}(x_1,...,x_n)\in\mathbb{R}^n$ is defined as $\|\boldsymbol{x}\|=(\sum_{j=1}^n|x_j|^2)^{\frac{1}{2}}$. For $\boldsymbol{x},\ \boldsymbol{y}\in\mathbb{R}^n$, $\boldsymbol{y}=\boldsymbol{x}\bmod 2\pi$ means $y_i\in\{x_i+2K_i\pi, K_i\in\mathcal{Z}\}$. Function $y=\text{module}(x,2\pi):\mathbb{R}\to[0,2\pi)$ is a function to return $y\in[0,2\pi)$ satisfying $y=x+2K\pi$ with some $K\in\mathcal{Z}$.

II. Preliminaries

A. Problem Formulation

Consider N unicycle-type vehicles in the form of

$$\dot{x}_i=v_i\cos\theta_i,\ \dot{y}_i=v_i\sin\theta_i,\ \dot{\theta}_i=\omega_i,\ i=1,2,...,N, \quad (1)$$

where $\boldsymbol{p}_i:=[x_i\ y_i]^{\mathrm{T}}\in\mathbb{R}^2$ is the absolute position and $\theta_i\in\mathbb{R}$ is the heading angle of each vehicle with respect to the inertial frame; see Fig. 1(a) for an illustration. $v_i\in\mathbb{R}$ and $\omega_i\in\mathbb{R}$ are its linear velocity and angular velocity respectively. Each vehicle is subject to the following physical velocity constraints [28]:

$$v_i\in[v_{\min},\ v_{\max}],\ \omega_i\in[-\omega_{\max},\ \omega_{\max}], \quad (2)$$

where $v_{\min}$, $v_{\max}$, and $\omega_{\max}$ are known positive constants as the bounds of the velocities.

In this note, the vehicles are required to converge to a circular formation where all vehicles travel along a common circle with a given center $\boldsymbol{p}_0=[x_0\ y_0]^{\mathrm{T}}$ and a desired radius $r>0$, orbit with a constant angular velocity ω_0 counterclockwise, and maintain a desired spacing described by a vector $\boldsymbol{\alpha}\in\mathbb{R}^N$ along the circle. The vector $\boldsymbol{\alpha}=\text{col}(\alpha_1,...,\alpha_N)$ is used to describe the desired separation angle of two vehicles with respect to the center. $\boldsymbol{\alpha}$ can be set as $\alpha_1=0$, $\alpha_N\le 2\pi$, and $\alpha_i\le\alpha_{i+1}$, $i=1,...,N-1$. Then, $\alpha_{ji}:=\alpha_j-\alpha_i$ can be viewed as the desired separation angle between vehicles i and j with respect to the center. Considering the velocity constraints (2), the constants ω_0 and r are assumed to satisfy

$$\omega_0 r\in(v_{\min},\ v_{\max}),\ \omega_0\in(0,\ \omega_{\max}). \quad (3)$$

Moreover, it is assumed that the communication devices are not available and each vehicle can only measure the relative information with respect to its neighbors in the sensor network. The topology of the sensor network is described by a sensor graph $\bar{\mathcal{G}}$ as follows. First, a directed graph $\mathcal{G}=(\mathcal{O},\mathcal{E})$ is used to model the sensor network of N vehicles. The directed graph $\mathcal{G}$ consists of a finite set of nodes $\mathcal{O}=\{1,...,N\}$ representing N vehicles, and a set of edges $\mathcal{E}\subseteq\{(j,i):j\ne i,i,j\in\mathcal{O}\}$ containing directed edges from node j to node i. Next, by combining $\mathcal{G}$ and node 0 (denoting the center $\boldsymbol{p}_0$), the sensor graph $\bar{\mathcal{G}}=(\bar{\mathcal{O}},\bar{\mathcal{E}})$ is obtained with $\bar{\mathcal{O}}=\mathcal{O}\cup\{0\}$ and $\bar{\mathcal{E}}=\mathcal{E}\cup\{(0,i),\ i\in\mathcal{O}\}$. A directed edge $(j,i)\in\bar{\mathcal{E}}$ means that vehicle i can measure the relative information with respect to vehicle j or the center. Define the sets $\mathcal{N}_i$ and $\bar{\mathcal{N}}_i$ as $\mathcal{N}_i=\{k\in\mathcal{O}|(k,i)\in\mathcal{E}\}$ and $\bar{\mathcal{N}}_i=\{j\in\bar{\mathcal{O}}|(j,i)\in\bar{\mathcal{E}}\}$ respectively.

Define $a_{ii}=0$ and $a_{ij}=1\iff(j,i)\in\mathcal{E}$. The Laplacian of graph $\mathcal{G}$ is denoted by $\mathcal{L}=[l_{ij}]\in\mathbb{R}^{N\times N}$, where $l_{ii}=\sum_{j=1}^N a_{ij}$ and $l_{ij}=-a_{ij}$ if $i\ne j$. Denote the Laplacian matrix of graph $\bar{\mathcal{G}}$ by $\bar{\mathcal{L}}$. Since not all vehicles have the knowledge of the center $\boldsymbol{p}_0$ in some practical scenarios, the following assumption is made on the sensor graph $\bar{\mathcal{G}}$:

Assumption 1: The directed graph $\bar{\mathcal{G}}$ contains a directed spanning tree with node 0 being the root. ■

In our setting, neither a global coordinate frame, i.e., the inertial frame, nor a common reference direction is required to be available. Thus, the absolute positions $\boldsymbol{p}_i$, $\boldsymbol{p}_j$, $j\in\bar{\mathcal{N}}_i$, or the relative positions $\boldsymbol{p}_i-\boldsymbol{p}_j$ cannot be measured. Each vehicle only uses its local coordinate frame, i.e., the Frenet-Serret frame, with the origin at its position $\boldsymbol{p}_i$ and the x-axis coincident with its orientation θ_i. Then, $\boldsymbol{p}_j$, $j\in\bar{\mathcal{N}}_i$, and θ_k, $k\in\mathcal{N}_i$, in the coordinate frame of vehicle i are expressed as

$$\boldsymbol{p}_j^i=[x_j^i\ y_j^i]^{\mathrm{T}}=\boldsymbol{R}(\theta_i)(\boldsymbol{p}_j-\boldsymbol{p}_i),\ \theta_k^i=\theta_k-\theta_i,$$

respectively, where $\boldsymbol{R}(\cdot)=\begin{bmatrix}\cos(\cdot) & \sin(\cdot)\\ -\sin(\cdot) & \cos(\cdot)\end{bmatrix}$. Besides, the separation angle between vehicles i and k with respect to the center is denoted by $\psi_{ki}:=\angle\boldsymbol{p}_i\boldsymbol{p}_0\boldsymbol{p}_k\in[0,2\pi)$, see Fig. 1(a) for illustration. The distance d_j^i and the bearing angle β_j^i are defined as follows

$$d_j^i=\|\boldsymbol{p}_j^i\|,\ \beta_j^i=\kappa(\boldsymbol{p}_j^i), \quad (4)$$

where $\kappa(\boldsymbol{p}_j^i)=0$ if $\boldsymbol{p}_j^i=\boldsymbol{0}$; otherwise $\kappa(\boldsymbol{p}_j^i)=\text{atan2}(y_j^i,x_j^i)$ with the two-argument arctangent function $\text{atan2}(\cdot):\mathbb{R}^2\backslash(0,0)\to[-\pi,\pi)$. $\boldsymbol{p}_j^i$ can be obtained by measuring d_j^i and β_j^i separately, see Fig. 1(a) for illustration.

However, it should be noted that $\boldsymbol{p}_j^i$ is unavailable when sensors cannot provide accurate distance measurements. For example, cameras along with markers can only measure the bearing and relative heading angles. The *circular formation control problem* formally defined as follows, is thus motivated.

Problem 1: Consider N nonholonomic vehicles in the form of (1). Given a center $\boldsymbol{p}_0\in\mathbb{R}^2$, a sensor graph $\bar{\mathcal{G}}$, and a constant vector $\boldsymbol{\alpha}\in\mathbb{R}^N$ describing the desired spacing, for vehicle i, $i=1,...,N$, with any initial states $[\boldsymbol{p}_i^{\mathrm{T}}(t_0)\ \theta_i(t_0)]^{\mathrm{T}}\in\mathbb{R}^3$, $\forall t_0\ge 0$, find a static controller using the information obtained from the onboard sensors, in the form of

$$[v_i\ \omega_i]^{\mathrm{T}}=\boldsymbol{\sigma}(\beta_j^i,\theta_k^i,r,\alpha_{ki},\omega_0),j\in\bar{\mathcal{N}}_i,k\in\mathcal{N}_i, \quad (5)$$

such that (i) $\lim_{t\to\infty}(\boldsymbol{p}_i(t)-\boldsymbol{p}_0)=r[\sin\theta_i(t)\ \ -\cos\theta_i(t)]^{\mathrm{T}}$, $\lim_{t\to\infty}\omega_i(t)=\omega_0$; (ii) $\lim_{t\to\infty}\psi_{ki}(t)-\alpha'_{ki}=0$, where ω_0 is a given positive constant, $\alpha'_{ki}=\text{module}(\alpha_{ki},2\pi)$ is a constant denoting the desired separation angle to the neighbors, and $\boldsymbol{\sigma}(\cdot)$ is a sufficiently smooth function. ■

Remark 2.1: As in [16], communication and direct distance measurements are not required in this work. Compared with [16] where the center has to be known to all vehicles, Assumption 1 only requires some (at least one) vehicles to have direct access to the knowledge of the center. ■

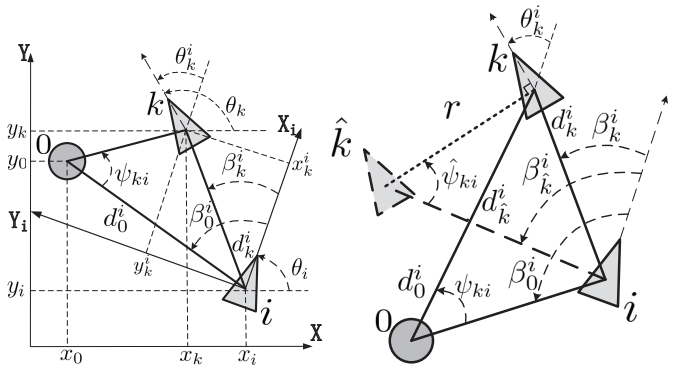

(a) Illustrations of the variables. (b) The "companion" vehicle $\hat{k}$.

Fig. 1. Illustration of the variables and the "companion" vehicle $\hat{k}$.

B. Technical Lemmas

We now review three technical lemmas which will be used in the next section.

The first lemma is on the stability of continuous-time adaptive systems [29].

Lemma 2.1: A system $\dot{\boldsymbol{x}} = \begin{bmatrix} A & -b\boldsymbol{u}^{\mathrm{T}}(t) \\ u(t)b^{\mathrm{T}} & 0 \end{bmatrix}$, where $\boldsymbol{x} = [\boldsymbol{x}_1^{\mathrm{T}}\ \boldsymbol{x}_2^{\mathrm{T}}]^{\mathrm{T}}$, $\boldsymbol{x}_1 \in \mathbb{R}^m$, $\boldsymbol{x}_2 \in \mathbb{R}^n$, $A \in \mathbb{R}^{m\times m}$ is an stable matrix with $A + A^{\mathrm{T}}$ being negative definite, (A, b) is controllable, and $\boldsymbol{u} : \mathbb{R}_{\geq 0} \to \mathbb{R}^n$ is piecewise-continuous and bounded. The equilibrium of this system is globally exponentially stable if and only if $\boldsymbol{u}(t)$ is persistently exciting, i.e., there exist positive constants t_0, T_0, and α such that $\int_t^{t+T_0} \boldsymbol{u}(\tau)\boldsymbol{u}^{\mathrm{T}}(\tau)d\tau \geq \alpha \boldsymbol{I},\ \forall t \geq t_0$. ■

The second lemma proposed in [30] is often referred to as the so-called reduction theorem for asymptotic stability of sets.

Lemma 2.2 (Proposition 14 in [30]): Consider a locally Lipschitz control system $\dot{\boldsymbol{\upsilon}} = \boldsymbol{f}(\boldsymbol{\upsilon}, \boldsymbol{\eta})$ with state space a domain $\Upsilon \in \mathbb{R}^q$, and assume that there exists a locally Lipschitz feedback $\bar{\boldsymbol{\eta}}(\boldsymbol{\upsilon})$ making the sets $\Gamma_n \subset \Gamma_{(n-1)} \subset \ldots \subset \Gamma_1$ positively invariant for the closed-loop system $\dot{\boldsymbol{\upsilon}} = \boldsymbol{f}(\boldsymbol{\upsilon}, \bar{\boldsymbol{\eta}}(\boldsymbol{\upsilon}))$. Let $\Gamma_0 := \Upsilon$, and if (i) for $i = 1, \ldots, n$, Γ_i is globally asymptotically stable relative to $\Gamma_{(i-1)}$ for the closed-loop system, (ii) all trajectories of the closed-loop system are bounded, and (iii) Γ_n is compact, then Γ_n is globally asymptotically stable for the closed-loop system. ■

Note that the definition of relative set stability can be referred to Definition 4 in [30].

The third lemma is Theorem 1 in [31].

Lemma 2.3: Suppose that Assumption 1 holds and the root node 0 in graph $\bar{\mathcal{G}}$ has no incoming edges from other nodes. Define $\mathcal{A} = \mathrm{diag}(a_{10}, \ldots, a_{N0})$, where $a_{i0} = 1$ if there is an edge $(0, i)$; $a_{i0} = 0$, otherwise. Let $\boldsymbol{\eta} = [\eta_1, \ldots, \eta_N]^{\mathrm{T}} = (\mathcal{L} + \mathcal{A})^{-1}\mathbf{1}_N$, $\boldsymbol{\zeta} = [\zeta_1, \ldots, \zeta_N]^{\mathrm{T}} = (\mathcal{L} + \mathcal{A})^{-\mathrm{T}}\mathbf{1}_N$, $P = \mathrm{diag}(p_1, \ldots, p_N)$ with $p_i = \zeta_i/\eta_i$, and $Q = P(\mathcal{L} + \mathcal{A}) + (\mathcal{L} + \mathcal{A})^{\mathrm{T}}P$. Then, P and Q are both positive definite. ■

III. Main Results

In this section, first a control strategy and a static controller are developed to solve the *circular formation control problem*. Then, stability analysis on the closed-loop system consisting of the proposed controller and the multi-vehicle system is given.

A. Controller Design

To achieve $\lim_{t\to\infty} \boldsymbol{p}_i(t) - \boldsymbol{p}_0 = r[\sin\theta_i(t)\ \ -\cos\theta_i(t)]^{\mathrm{T}}$, it suffices to achieve

$$\lim_{t\to\infty} d_0^i(t) = r,\ \lim_{t\to\infty} \beta_0^i(t) = \frac{\pi}{2}. \tag{6}$$

The dynamics of d_0^i and β_0^i can be described as

$$\dot{d}_0^i = -v_i\cos\beta_0^i,\ \ \dot{\beta}_0^i = -\omega_i + v_i\frac{\sin\beta_0^i}{d_0^i}, \tag{7}$$

for $[d_0^i\ \ \beta_0^i]^{\mathrm{T}} \in (0, +\infty) \times [-\pi, \pi)$.

According to $\psi_{ki} = \mathrm{module}(\mathrm{atan2}(y_k - y_0, x_k - x_0) - \mathrm{atan2}(y_i - y_0, x_i - x_0), 2\pi)$, the dynamics of ψ_{ki} are

$$\dot{\psi}_{ki} = \frac{v_k\sin\beta_0^k}{d_0^k} - \frac{v_i\sin\beta_0^i}{d_0^i},\ \ k \in \mathcal{N}_i, \tag{8}$$

for $\psi_{ki} \in [0, 2\pi)$.

However, not all vehicles know the center, and they can only sense its neighbors. In this case, we develop a control strategy as follows.

Each neighbor of vehicle i, i.e., vehicle k, $k \in \mathcal{N}_i$, is assigned a virtual "companion" vehicle, namely vehicle $\hat{k}$. The position of vehicle $\hat{k}$ is located on the coordinate $(0, r)$ in the coordinate frame of vehicle k, i.e., $\boldsymbol{p}_{\hat{k}}^k = [0\ \ r]^{\mathrm{T}}$. If vehicle i can sense the relative heading angle θ_k^i, then it can detect vehicle $\hat{k}$ and measure the bearing angle $\beta_{\hat{k}}^i \in [-\pi, \pi)$, see Fig. 1(b) for illustration. The "companion" vehicles are only used by vehicles which do not know the center, and serve as the estimates for the centers of the neighbors. Vehicles which know the center do not need to use the estimate $\beta_{\hat{k}}^i$.

Then, a static controller is proposed for each vehicle i as

$$v_i = \omega_0 r + c_1 r\tanh(\mu\sum_{k\in\mathcal{N}_i}(2\beta_k^i - \alpha'_{ki})), \tag{9}$$

$$\omega_i = \frac{v_i}{r} - c_2\cos(b_i\beta_0^i + a_i\sum_{k\in\mathcal{N}_i}\beta_{\hat{k}}^i), \tag{10}$$

where $\alpha'_{ki} = \mathrm{module}(\alpha_{ki}, 2\pi)$, $b_i = 1$ and $a_i = 0$ if $(0, i) \in \bar{\mathcal{E}}$; $b_i = 0$ and $a_i = 1/\|\mathcal{N}_i\|$, otherwise. $\|\mathcal{N}_i\|$ denotes the number of the neighboring vehicles, and μ is any positive constant. Moreover, c_1 and c_2 are positive constants satisfying

$$c_1 \in (0, \sigma),\ \ c_2 \in (0, \omega_{\max} - \omega_0 - c_1], \tag{11}$$

with $\sigma = \min(\frac{v_{\max}}{r} - \omega_0, \omega_0 - \frac{v_{\min}}{r}, \omega_{\max} - \omega_0)$.

To implement the proposed controller (9)–(10), each vehicle is required to be equipped with an omnidirectional monocular camera and visual markers for being observed by its neighbors. As shown in [27], each vehicle i can use the onboard camera to detect the visual markers on its neighbors. The bearing angles β_j^i, $j \in \bar{\mathcal{N}}_i$, and the relative heading angles θ_k^i, $k \in \mathcal{N}_i$, can be directly measured. For vehicle i, we suggest the following two methods to detect a virtual "companion" vehicle $\hat{k}$.

The first method requires vehicle i to capture an image $\mathcal{I}(t_0)$ at the initial instant and do a one-time calibration in $\mathcal{I}(t_0)$ as a reference. At the initial instant t_0, vehicle i first captures the size of the visual marker on vehicle k, i.e., $m_k(t_0)$, and calibrates a distance $r_k(t_0)$ for the radius r corresponding to the size of the visual marker $m_k(t_0)$. Set several virtual

"rulers" with length $r_k(t_0)$ and orientation perpendicular to $\theta_k(t_0)$. Let the ends of these "rulers" be attached to each feature point of the visual marker. Then, the tops of the "rulers" form a virtual marker in $\mathcal{I}(t_0)$ and this virtual marker is used to measure $\beta^i_{\hat{k}}(t_0)$. To measure $\beta^i_{\hat{k}}(t)$, $t \geq t_0$, in the same way, the remaining issue is to find the virtual marker in an image $\mathcal{I}(t)$ captured at instant t and to determine the length of the "rulers" $r_k(t)$ in $\mathcal{I}(t)$. Note that from t_0 onwards, $r_k(t)$ and the size of the visual marker $m_k(t)$ in $\mathcal{I}(t)$ are influenced by the rotation and translation of the two vehicles, and $m_k(t)$ can be measured by observing the marker. Since ω_i and θ^i_k are known, $\theta_k(t) - \theta_i(t_0)$ can be computed. Then, image $\mathcal{I}(t)$ can be rotated to the same orientation as $\mathcal{I}(t_0)$, and an image $\mathcal{I}'(t)$ can be obtained. Thus, the size of the visual marker $m'_k(t)$ in image $\mathcal{I}'(t)$ can be computed. Compared with $\mathcal{I}(t_0)$, $\mathcal{I}'(t)$ is only influenced by the translation of the two vehicles. Using the proportion $\frac{m'_k(t)}{m_k(t_0)} = \frac{r'_k(t)}{r_k(t_0)}$, $r'_k(t)$ in $\mathcal{I}'(t)$ can be computed. Finally, by rotating $\mathcal{I}'(t)$ back to the same orientation as $\mathcal{I}(t)$, $r_k(t)$ can be determined and the virtual marker can be found in $\mathcal{I}(t)$. Noting that the visual marker and its corresponding virtual marker are always in the same plane perpendicular to the ground, the implementation method described above does not require the camera to acquire the depth information, and the monocular camera can be used.

The second method also uses the monocular camera, and additionally requires each vehicle to install a small laser transmitter, such as a low-cost laser pointer or laser pen. The laser transmitter is fixed on the top of vehicle k and projects a pattern with length r and orientation perpendicular to $\theta_k(t)$, onto the ground or the ceiling. Instead of the computed virtual marker described in the first method, the projected pattern serves as a visual marker on the "companion" vehicle $\hat{k}$, such that vehicle i is able to detect it and to measure the bearing angle $\beta^i_{\hat{k}}$. Note that the projected patterns and the visual marker generally have unknown sizes and known scales, such as an equilateral triangle with unknown side length. The style of the projected pattern can be set the same as the visual marker of the corresponding vehicle. In this way, the size of the visual marker is not required to be known and the relative heading angle measurements are not needed. Thus, the proposed approach can be implemented with pure bearing angle measurements.

Even if the sensing capability of the vehicle is very limited and cannot provide any relative measurements, such as *e-puck* robots used in in [16], the required measurements can be provided by one calibrated overhead camera and direct distance measurements are still not required. The implementation can be carried out as shown in the experiments in [8, 16] where circular formation control laws with bearing angle measurements were developed.

B. Main Theorem

Now, the main result of this note is stated as follows.

Theorem 3.1: Controller (9)–(10) solves the *circular formation control problem*, i.e., Problem 1, if Assumption 1 and the following Assumptions 2–3 are satisfied.

Assumption 2: Graph $\mathcal{G}$ contains a directed spanning tree with a root node to which there exist no directed edges from other nodes. ■

Assumption 3: A subgraph of graph $\bar{\mathcal{G}}$, $\bar{\mathcal{G}}' = (\bar{\mathcal{O}}, \bar{\mathcal{E}}')$ with $\bar{\mathcal{E}}' = \bar{\mathcal{E}} \setminus \{(j,i) | j \in \mathcal{O}, i \in \{i \in \mathcal{O} | (0,i) \in \bar{\mathcal{E}}\}\}$ contains no directed cycles. ■

Moreover, velocity constraints (2) can always be satisfied. ■

Subgraph $\bar{\mathcal{G}}'$ is obtained by removing the edges (j,i), $j \in \mathcal{O}$, $i \in \{i \in \mathcal{O} | (0,i) \in \bar{\mathcal{E}}\}$, in sensor graph $\bar{\mathcal{G}}$, which corresponds to the design of a_i and b_i in (10).

In what follows, Theorem 3.1 will be proved by using mathematical induction and Lemma 2.2. The following two steps will be presented.

The first step is to show that all the vehicles subject to velocity constraints (2) can converge to the circular motion along the common circle with the center $\boldsymbol{p}_0$ and radius r.

The second step is to show that the vehicles traveling along this common circle can converge to the desired spacing.

Denote $\boldsymbol{d}_0 = \text{col}(d^1_0, ..., d^N_0)$, $\boldsymbol{\beta}_0 = \text{col}(\beta^1_0, ..., \beta^N_0)$, and $\boldsymbol{\psi} = \text{col}(\psi_{k_1 1}, ..., \psi_{j_1 1}, ..., \psi_{k_N N}, ..., \psi_{j_N N})$, $k_i \leq j_i$, $k_i,\ j_i \in \mathcal{N}_i$. Define $\Pi = [0, +\infty)^N \times [-\pi, \pi)^N \times [0, 2\pi)^{\|\mathcal{E}\|}$, where $\|\mathcal{E}\|$ denotes the number of edges in graph $\mathcal{G}$. The aforementioned two steps can be rephrased as follows.

Step 1: To stabilize the following set Γ_1 relative to Π,

$$\Gamma_1 = \{[\boldsymbol{d}_0^{\mathrm{T}}\ \boldsymbol{\beta}_0^{\mathrm{T}}\ \boldsymbol{\psi}^{\mathrm{T}}]^{\mathrm{T}} \in \Pi : d^i_0 = r, \beta^i_0 = \frac{\pi}{2}, i \in \mathcal{O}\}. \quad (12)$$

Step 2: To stabilize the following set Γ_2 relative to Γ_1,

$$\Gamma_2 = \{[\boldsymbol{d}_0^{\mathrm{T}}\ \boldsymbol{\beta}_0^{\mathrm{T}}\ \boldsymbol{\psi}^{\mathrm{T}}]^{\mathrm{T}} \in \Gamma_1 : \psi_{ki} = \alpha'_{ki}, i \in \mathcal{O}, k \in \mathcal{N}_i\}. \quad (13)$$

C. Convergence to the Common Circle

The objective of this step is to show that $[d^i_0\ \beta^i_0]^{\mathrm{T}} = [r\ \frac{\pi}{2}]^{\mathrm{T}}$ is asymptotically stable for the closed-loop system consisting of system (7) and controller (9)–(10).

It follows from (9) and (10) that $v_i \in (\omega_0 r - c_1 r,\ \omega_0 r + c_1 r)$ and $\omega_i \in [\omega_0 - c_1 - c_2,\ \omega_0 + c_1 + c_2]$. To satisfy velocity constraints (2), the positive constants c_1 and c_2 need to meet

$$\begin{aligned} &\omega_0 + c_1 + c_2 \leq \omega_{\max},\ \omega_0 - c_1 - c_2 \geq -\omega_{\max}, \\ &\omega_0 r + c_1 r \leq v_{\max},\ \omega_0 r - c_1 r \geq v_{\min}. \end{aligned} \quad (14)$$

Using (3) and (11), it can be checked that the inequalities in (14) are met. Thus, controller (9)–(10) ensures that velocity constraints (2) are satisfied.

For the vehicles which do not know the center, i.e., vehicle i, $i \in \mathcal{O} \setminus \{i \in \mathcal{O} | (0,i) \in \bar{\mathcal{E}}\}$, ω_i in (10) becomes

$$\omega_i = \frac{v_i}{r} - c_2 \cos\Big(\frac{1}{\|\mathcal{N}_i\|} \sum_{k \in \mathcal{N}_i} \beta^i_{\hat{k}}\Big). \quad (15)$$

While for the vehicles which know the center, i.e., vehicle i, $i \in \{i \in \mathcal{O} | (0,i) \in \bar{\mathcal{E}}\}$, ω_i in (10) becomes

$$\omega_i = \frac{v_i}{r} - c_2 \cos \beta^i_0. \quad (16)$$

It can be observed that the information measured through the directed edges (j,i), $j \in \mathcal{O}$, $i \in \{i \in \mathcal{O} | (0,i) \in \bar{\mathcal{E}}\}$, in the sensor graph $\bar{\mathcal{G}}$ is not used in the controller design for ω_i. Thus, graph $\bar{\mathcal{G}}'$ which excludes these edges, is used for the following analysis.

Under Assumptions 1 and 3, graph $\bar{\mathcal{G}}' = (\bar{\mathcal{O}}, \bar{\mathcal{E}}')$ contains a directed spanning tree with node 0 being the root and contains no directed cycles. Then, graph $\bar{\mathcal{G}}'$ can be further divided into $M+1$ ($M \geq 1$) sequential subgraphs $\bar{\mathcal{G}}'_0$, $\bar{\mathcal{G}}'_1$, ..., $\bar{\mathcal{G}}'_M$. Denote $\bar{\mathcal{O}}_m$ as the set which includes the nodes in subgraph $\bar{\mathcal{G}}'_m$, $m = 0, ..., M$. In subgraph $\bar{\mathcal{G}}'_0$, there exists only node 0, i.e., $\bar{\mathcal{O}}_0 = \{0\}$. Inside each subgraph, there exist no edges. There exist directed edges only from the nodes in some of the subgraphs $\bar{\mathcal{G}}'_0$,..., $\bar{\mathcal{G}}'_m$, $m = 0, 1, ..., M-1$, to the nodes in subgraph $\bar{\mathcal{G}}'_{(m+1)}$, i.e., $\bar{\mathcal{E}}' = \{(j,i) | i \in \bar{\mathcal{O}}_{(m+1)}, m = 0, 1, ..., M-1, j \in \bar{\mathcal{O}}_n, 0 \leq n \leq m\}$.

In what follows, mathematical induction is used to prove that vehicle i, $i \in \bar{\mathcal{O}}_m$, $m = 1, 2, ..., M$, can converge to the common circle with center $\boldsymbol{p}_0$, i.e., (6) can be achieved.

First, we show that (6) holds for vehicle i, $i \in \bar{\mathcal{O}}_1$. Define $\boldsymbol{\xi}_i = [d_0^i \ \beta_0^i]^{\mathrm{T}}$. The closed-loop system consisting of system (7) and controller (16) becomes

$$\dot{\boldsymbol{\xi}}_i = \boldsymbol{f}_i(\boldsymbol{\xi}_i, t), \ \boldsymbol{\xi}_i \in (0, +\infty) \times [-\pi, \pi), \tag{17}$$

where

$$\boldsymbol{f}_i(\boldsymbol{\xi}_i, t) = \begin{bmatrix} -v_i \cos\beta_0^i \\ -\frac{v_i}{r} + c_2 \cos\beta_0^i + v_i \frac{\sin\beta_0^i}{d_0^i} \end{bmatrix}. \tag{18}$$

Consider a Lyapunov function candidate

$$V_i(\boldsymbol{\xi}_i) = \frac{1}{2}(d_0^i \cos\beta_0^i)^2 + \frac{1}{2}(d_0^i \sin\beta_0^i - r)^2. \tag{19}$$

$V_i(\boldsymbol{\xi}_i(t))$ is continuous but not continuously differentiable at an instant $t_\epsilon \geq t_0$ when $d_0^i(t_\epsilon) = 0$. It follows from the definition of the bearing angle in (4) and (9)–(10) that controller (9)–(10) is still working at instant t_ϵ, and $v_i(t) \geq v_{\min} > 0$ holds for all $t \geq t_0$. Then, $\frac{\mathrm{d}(\boldsymbol{p}_i - \boldsymbol{p}_0)}{\mathrm{d}t} \neq 0$ for all $t \geq t_0$, and the state $\boldsymbol{p}_0^i = \boldsymbol{0}$, i.e., $d_0^i = 0$ will not be maintained even if there exists an instant instant t_ϵ when $d_0^i(t_\epsilon) = 0$. Thus, $V_i(\boldsymbol{\xi}_i(t))$ is piecewise continuously differentiable along the solutions of system (17). Motivated by [32], the upper right-hand time derivative of $V_i(\boldsymbol{\xi}_i)$, i.e., $\mathrm{D}^+V_i(\boldsymbol{\xi}_i)$ can be used for analysis in this case.

Taking the upper right-hand time derivative of (19) along the trajectories of system (17) yields

$$\begin{aligned}
\mathrm{D}^+V_i(\boldsymbol{\xi}_i) &= -d_0^i \cos\beta_0^i (v_i \cos^2\beta_0^i + d_0^i \dot{\beta}_0^i \sin\beta_0^i) \\
&\quad + (d_0^i \sin\beta_0^i - r)(d_0^i \dot{\beta}_0^i \cos\beta_0^i - v_i \cos\beta_0^i \sin\beta_0^i) \\
&= -v_i d_0^i \cos\beta_0^i + v_i r \cos\beta_0^i \sin\beta_0^i \\
&\quad + d_0^i r \cos\beta_0^i (\frac{v_i}{r} - c_2 \cos\beta_0^i - \frac{v_i \sin\beta_0^i}{d_0^i}) \\
&= -c_2 r d_0^i \cos^2\beta_0^i \leq 0.
\end{aligned} \tag{20}$$

Then, the equilibrium set $S_i = \{\boldsymbol{\xi}_i | \mathrm{D}^+V_i(\boldsymbol{\xi}_i) = 0\}$ is globally stable relative to $[0, +\infty) \times [-\pi, \pi)$, and $\mathrm{D}^+V_i(\boldsymbol{\xi}_i) = 0$ implies $d_0^i \cos^2\beta_0^i = 0$. Since $d_0^i = 0$ cannot be maintained, it can be concluded that $\cos\beta_0^i(t) \to 0$ as $t \to \infty$. It follows from $\dot{d}_0^i = -v_i \cos\beta_0^i$ that $d_0^i(t)$ converges to a constant. Besides, $\cos\beta_0^i(t) \to 0$ implies $\dot{\beta}_0^i(t) \to 0$ and $\beta_0^i(t) \to \frac{\pi}{2}$ or $-\frac{\pi}{2}$. Then, it follows from $\dot{\beta}_0^i(t) \to 0$ and $\dot{\beta}_0^i = -\frac{v_i}{r} + c_2 \cos\beta_0^i + v_i \frac{\sin\beta_0^i}{d_0^i}$ that $-\frac{v_i(t)}{r} + \frac{v_i(t)\sin\beta_0^i(t)}{d_0^i(t)} \to 0$. Since $d_0^i \geq 0$, $v_i \geq v_{\min} > 0$, and d_0^i converges to a constant, only $\beta_0^i(t) \to \frac{\pi}{2}$ and $d_0^i(t) \to r$ would yield $-\frac{v_i(t)}{r} + \frac{v_i(t)\sin\beta_0^i(t)}{d_0^i(t)} \to 0$. Thus, $\beta_0^i(t)$ goes to $\frac{\pi}{2}$ and the equilibrium set $S_i = \{\boldsymbol{\xi}_i | \boldsymbol{\xi}_i = [r \ \frac{\pi}{2}]^{\mathrm{T}}\}$ is globally asymptotically stable relative to $[0, +\infty) \times [-\pi, \pi)$.

Therefore, (6) is achieved for vehicle i, $i \in \bar{\mathcal{O}}_1$, which is summarized in the following proposition.

Proposition 3.1: Consider a system in the form of (17). For any $\boldsymbol{\xi}_i \in (0, +\infty) \times [-\pi, \pi)$, the equilibrium point $\boldsymbol{\xi}_i = [r \ \frac{\pi}{2}]^{\mathrm{T}}$ is asymptotically stable for system (17). ■

Second, supposing that the vehicle k, $k \in \bar{\mathcal{O}}_m$, $1 \leq m \leq M-1$, can converge to the common circle with center $\boldsymbol{p}_0$ and radius r, i.e. $\lim_{t\to\infty} \boldsymbol{\xi}_k(t) = [r \ \frac{\pi}{2}]^{\mathrm{T}}$, we prove that for $i \in \bar{\mathcal{O}}_{(m+1)}$, $\lim_{t\to\infty} \boldsymbol{\xi}_i(t) = [r \ \frac{\pi}{2}]^{\mathrm{T}}$.

Define $\tilde{\boldsymbol{\xi}}_i := [\tilde{d}_0^i \ \tilde{\beta}_0^i]^{\mathrm{T}} = \boldsymbol{\xi}_i - [r \ \frac{\pi}{2}]^{\mathrm{T}}$. The closed-loop system consisting of system (7) and controller (15) can be written in the following form

$$\dot{\tilde{\boldsymbol{\xi}}}_i = \tilde{\boldsymbol{f}}_i(\tilde{\boldsymbol{\xi}}_i, t) + \boldsymbol{g}_i(\tilde{\boldsymbol{\xi}}_i, t), \ \tilde{\boldsymbol{\xi}}_i \in (-r, +\infty) \times [-\frac{3\pi}{2}, \frac{\pi}{2}), \tag{21}$$

where

$$\tilde{\boldsymbol{f}}_i(\tilde{\boldsymbol{\xi}}_i, t) = \begin{bmatrix} v_i \sin\tilde{\beta}_0^i \\ -\frac{v_i}{r} - c_2 \sin\tilde{\beta}_0^i + v_i \frac{\cos\tilde{\beta}_0^i}{\tilde{d}_0^i + r} \end{bmatrix}, \tag{22}$$

$$\boldsymbol{g}_i(\tilde{\boldsymbol{\xi}}_i, t) = c_2 \begin{bmatrix} 0 & \cos(\frac{1}{\|\mathcal{N}_i\|} \sum_{k \in \mathcal{N}_i} \beta_{\hat{k}}^i) + \sin\tilde{\beta}_0^i \end{bmatrix}^{\mathrm{T}}. \tag{23}$$

System (21) can be viewed as a nominal system $\dot{\tilde{\boldsymbol{\xi}}}_i = \tilde{\boldsymbol{f}}_i(\tilde{\boldsymbol{\xi}}_i, t)$ with the perturbation $\boldsymbol{g}_i(\tilde{\boldsymbol{\xi}}_i, t)$. Furthermore, using Proposition 3.1 yields $\tilde{\boldsymbol{\xi}}_i = \boldsymbol{0}$ is asymptotically stable for the nominal system $\dot{\tilde{\boldsymbol{\xi}}}_i = \tilde{\boldsymbol{f}}_i(\tilde{\boldsymbol{\xi}}_i, t)$.

Then, we further study the convergence rate of the nominal system $\dot{\tilde{\boldsymbol{\xi}}}_i = \tilde{\boldsymbol{f}}_i(\tilde{\boldsymbol{\xi}}_i, t)$. Define $\boldsymbol{p}_{ei} = [d_0^i \cos\beta_0^i \ d_0^i \sin\beta_0^i - r]^{\mathrm{T}}$. Note that $\boldsymbol{p}_{ei} = \boldsymbol{0}$ if and only if $[d_0^i(t) \ \beta_0^i(t)]^{\mathrm{T}} = [r \ \frac{\pi}{2}]^{\mathrm{T}}$. Consider the case with $\boldsymbol{g}_i(\tilde{\boldsymbol{\xi}}_i, t) = 0$, it follows from (22) that

$$\begin{aligned}
\dot{\boldsymbol{p}}_{ei} &= A_i(t)\boldsymbol{p}_{ei} + \varepsilon_i(t)\boldsymbol{p}_{ei}, \ A_i(t) = \begin{bmatrix} -c_2 & \frac{v_i(t)}{r} \\ -\frac{v_i(t)}{r} & 0 \end{bmatrix}, \\
\varepsilon_i(t) &= c_2 \begin{bmatrix} 1 - \frac{r}{d_0^i(t)} & -\cos\beta_0^i(t) \\ \cos\beta_0^i(t) & 0 \end{bmatrix}.
\end{aligned} \tag{24}$$

By Lemma 2.1, (2), and (9), $\boldsymbol{p}_{ei} = \boldsymbol{0}$ of the system $\dot{\boldsymbol{p}}_{ei} = A_i(t)\boldsymbol{p}_{ei}$ is globally exponentially stable. Since $\tilde{\boldsymbol{\xi}}_i = \boldsymbol{0}$ is asymptotically stable for the nominal system $\dot{\tilde{\boldsymbol{\xi}}}_i = \tilde{\boldsymbol{f}}_i(\tilde{\boldsymbol{\xi}}_i, t)$, then $\varepsilon_i(t)$ converges to zero as $t \to \infty$. It follows from [33, Corollary 9.1 and Lemma 9.5] that $\boldsymbol{p}_{ei} = \boldsymbol{0}$ of system (24) is globally exponentially stable. Thus, the nominal system $\dot{\tilde{\boldsymbol{\xi}}}_i = \tilde{\boldsymbol{f}}_i(\tilde{\boldsymbol{\xi}}_i, t)$ is exponentially stable at $\tilde{\boldsymbol{\xi}}_i = \boldsymbol{0}$.

Next, we show $\lim_{t\to\infty} (\cos(\frac{1}{\|\mathcal{N}_i\|} \sum_{k \in \mathcal{N}_i} \beta_{\hat{k}}^i(t)) - \cos\beta_0^i(t)) = 0$, i.e., $\lim_{t\to\infty} \boldsymbol{g}_i(\tilde{\boldsymbol{\xi}}_i, t) = \boldsymbol{0}$, for any $\beta_{\hat{k}}^i$, $\beta_0^i \in [-\pi, \pi)$, $k \in \bar{\mathcal{O}}_m$, $i \in \bar{\mathcal{O}}_{(m+1)}$, $1 \leq m \leq M-1$.

By the definition of the bearing angle in (4), $\beta_{\hat{k}}^i$ and β_0^i can be expressed as

$$\beta_{\hat{k}}^i = \kappa(\boldsymbol{p}_{\hat{k}}^i), \ \beta_0^i = \kappa(\boldsymbol{p}_0^i). \tag{25}$$

According to the position of vehicle $\hat{k}$ (see Fig. 1(b) for

illustration), $\boldsymbol{p}_{\hat{k}}^i$ can be expressed as

$$\boldsymbol{p}_{\hat{k}}^i = \boldsymbol{p}_k^i + \boldsymbol{R}(-\theta_k^i)\boldsymbol{p}_{\hat{k}}^k,\ \boldsymbol{p}_{\hat{k}}^k = [0 \quad r]^{\mathrm{T}}. \tag{26}$$

Besides, $\boldsymbol{p}_0^i$ can be expressed as

$$\boldsymbol{p}_0^i = \boldsymbol{p}_k^i + \boldsymbol{R}(-\theta_k^i)\boldsymbol{p}_0^k,\ \boldsymbol{p}_0^k = [d_0^k\cos\beta_0^k\ \ d_0^k\sin\beta_0^k]^{\mathrm{T}}. \tag{27}$$

Since $\lim_{t\to\infty}[d_0^k(t)\ \beta_0^k(t)]^{\mathrm{T}} = [r\ \frac{\pi}{2}]^{\mathrm{T}}$, it follows from (26) and (27) that $\lim_{t\to\infty}(\boldsymbol{p}_k^i(t) - \boldsymbol{p}_0^i(t)) = \boldsymbol{0}$.

Then, by (25), $\lim_{t\to\infty}(\beta_{\hat{k}}^i(t) - \beta_0^i(t)) = 0$, and thus

$$\lim_{t\to\infty} \boldsymbol{g}_i(\tilde{\boldsymbol{\xi}}_i, t) = \boldsymbol{0}. \tag{28}$$

Since $\tilde{\boldsymbol{\xi}}_i = \boldsymbol{0}$ is exponentially stable for the nominal system $\dot{\tilde{\boldsymbol{\xi}}}_i = \tilde{\boldsymbol{f}}_i(\tilde{\boldsymbol{\xi}}_i, t)$ and (28) holds, then by [33, Corollary 9.1 and Lemma 9.5], $\tilde{\boldsymbol{\xi}}_i = \boldsymbol{0}$ is asymptotically stable for system (21) with $i \in \bar{\mathcal{O}}_{(m+1)}$.

Hence, (6) can be achieved for all vehicles. All these arguments are summarized in the following proposition.

Proposition 3.2: Consider N systems in the form of (7) and a sensor graph $\bar{\mathcal{G}}$ under Assumptions 1 and 3. Controllers (9)–(10) ensure that velocity constraints (2) are satisfied and $\lim_{t\to\infty}[d_0^i(t)\ \beta_0^i(t)]^{\mathrm{T}} = [r\ \frac{\pi}{2}]^{\mathrm{T}}$, $i \in \mathcal{O}$, for any $[d_0^i(t_0)\ \beta_0^i(t_0)]^{\mathrm{T}} \in (0, +\infty) \times [-\pi, \pi)$, i.e., Γ_1 is globally asymptotically stable relative to Π. ■

D. Convergence to the Desired Spacing

The objective of this step is to show that vehicles traveling along the common circle can converge to the desired spacing, i.e., ψ_{ki} converges to α'_{ki} for each vehicle i.

When all the vehicles locate on the common circle, i.e., $d_0^i(t) = r$ and $\beta_0^i(t) = \frac{\pi}{2}$, $i \in \mathcal{O}$, then $\beta_{\hat{k}}^i = \beta_0^i$, $k \in \mathcal{N}_i$, and the separation angle ψ_{ki} satisfies

$$\psi_{ki} = 2\beta_k^i,\ \theta_k - \theta_i = \psi_{ki} \bmod 2\pi. \tag{29}$$

By Assumption 2 and Lemma 3.3 in [34], the Laplacian matrix $\mathcal{L}$ of graph $\mathcal{G}$ has a simple eigenvalue 0, and the corresponding right eigenvector is $\boldsymbol{1}_N$. Then, $\ker(\mathcal{L}) = \operatorname{span}\boldsymbol{1}_N$. Denoting $\boldsymbol{\theta} = \operatorname{col}(\theta_1, ..., \theta_N)$ and using $\theta_k - \theta_i = \psi_{ki} \bmod 2\pi$, $i \in \mathcal{O}$, $k \in \mathcal{N}_i$, yields

$$\begin{aligned}\{\boldsymbol{\psi}|\psi_{ki} = \alpha'_{ki}\} &= \{\boldsymbol{\psi}|\theta_k - \theta_i = (\alpha_k - \alpha_i) \bmod 2\pi\}\\ &= \{\boldsymbol{\psi}|\theta_1 - \alpha_1 \bmod 2\pi = ... = \theta_N - \alpha_N \bmod 2\pi\}\\ &= \{\boldsymbol{\psi}|\mathcal{L}(\boldsymbol{\theta} - \boldsymbol{\alpha}) = \boldsymbol{0}_N \bmod 2\pi\}.\end{aligned}$$

Thus, to show $\lim_{t\to\infty}\psi_{ki}(t) - \alpha'_{ki} = 0$, for each $i \in \mathcal{O}$, $k \in \mathcal{N}_i$, it suffices to show that $\lim_{t\to\infty}\mathcal{L}(\boldsymbol{\theta}(t) - \boldsymbol{\alpha}) = \boldsymbol{0}_N \bmod 2\pi$.

Define $\gamma_i = \mu\sum_{k\in\mathcal{N}_i}(\psi_{ki} - \alpha'_{ki})$. Denote $\boldsymbol{\gamma} = \operatorname{col}(\gamma_1, ..., \gamma_N)$ and using (29) leads to

$$\boldsymbol{\gamma} \bmod 2\pi = \mathcal{L}(\boldsymbol{\theta} - \boldsymbol{\alpha}). \tag{30}$$

Moreover, it follows from (8), (9), (29), $d_0^i(t) = r$ and $\beta_0^i(t) = \frac{\pi}{2}$ that the dynamics of γ_i can be written as

$$\dot{\gamma}_i = c_1\mu\sum_{k\in\mathcal{N}_i}(\tanh\gamma_k - \tanh\gamma_i). \tag{31}$$

Under Assumption 2, let node 1 be the root node with no incoming edges, and $\gamma_1 = 0$ and $\dot{\gamma}_1 = 0$. Denote $\underline{\mathcal{L}}$ as the Laplacian matrix of a subgraph $\underline{\mathcal{G}} = (\mathcal{O}\setminus\{1\}, \mathcal{E})$, and define a diagonal matrix $\underline{\mathcal{A}} = \operatorname{diag}(a_{21}, ..., a_{N1})$, where $a_{i1} = 1$ if there is an edge $(1, i)$; $a_{i1} = 0$, otherwise. Define

$$\tilde{\gamma}_i = \gamma_i - \gamma_1,\ \Lambda_i = \tanh\tilde{\gamma}_i,\ i \geq 2, \tag{32}$$

and denote $\boldsymbol{\Lambda} = \operatorname{col}(\Lambda_2, ..., \Lambda_N)$. The dynamics of $\boldsymbol{\Lambda}$ can be written in the following compact form:

$$\dot{\boldsymbol{\Lambda}} = -c_1\mu\underline{W}(\boldsymbol{\Lambda})(\underline{\mathcal{L}} + \underline{\mathcal{A}})\boldsymbol{\Lambda}, \tag{33}$$

where $\underline{W}(\boldsymbol{\Lambda}) = \operatorname{diag}(1-\Lambda_2^2, ..., 1-\Lambda_N^2)$. Since $\tanh(\cdot) \in (-1, 1)$, $\Lambda_i \in (-1, 1)$ and $\underline{W}(\boldsymbol{\Lambda})$ is positive definite. Define $\boldsymbol{\eta} = [\eta_2, ..., \eta_N]^{\mathrm{T}} = (\underline{\mathcal{L}} + \underline{\mathcal{A}})^{-1}\boldsymbol{1}_N$, $\boldsymbol{\zeta} = [\zeta_2, ..., \zeta_N]^{\mathrm{T}} = (\underline{\mathcal{L}} + \underline{\mathcal{A}})^{-\mathrm{T}}\boldsymbol{1}_N$, and $P = \operatorname{diag}(p_2, ..., p_N)$ with $p_i = \zeta_i/\eta_i$, $i \geq 2$. By Lemma 2.3, P is positive definite.

Furthermore, define $W(\boldsymbol{\Lambda}) = \operatorname{diag}(w_2, ..., w_N)$, where $w_i = f(\Lambda_i) : (-1, 1) \to \mathbb{R}$, $i \geq 2$, and $f(\cdot)$ is defined as

$$f(x) = \begin{cases} \frac{1}{x^2}h(x), & x \in (-1, 1)\setminus\{0\},\\ 1, & x = 0,\end{cases}, \tag{34}$$

with $h(\cdot) : (-1, 1) \to \mathbb{R}$ satisfying $\frac{\partial h(x)}{\partial x} = \frac{2x}{1-x^2}$.

By L'Hospital's rule, $\lim_{x\to 0} = 1 = f(0)$, and $f(x)$ is a differentiable function satisfying

$$f(x)(1-x^2) + \frac{\partial f(x)}{2\partial x}(1-x^2)x = 1. \tag{35}$$

Using (35), it can be verified that $f(x) > 0$ for $x \in (-1, 1)$.

Then, consider the following Lyapunov function candidate

$$V(\boldsymbol{\Lambda}) = \frac{1}{2}\boldsymbol{\Lambda}^{\mathrm{T}}PW(\boldsymbol{\Lambda})\boldsymbol{\Lambda}, \tag{36}$$

and its time derivative along the trajectories of system (33) is

$$\begin{aligned}\dot{V}(\boldsymbol{\Lambda}) &= -c_1\mu\boldsymbol{\Lambda}^{\mathrm{T}}(PW\underline{W}(\underline{\mathcal{L}} + \underline{\mathcal{A}}) + (\underline{\mathcal{L}} + \underline{\mathcal{A}})^{\mathrm{T}}\underline{W}PW)\boldsymbol{\Lambda}\\ &\quad + c_1\mu\sum_{i=2}^{N}(p_i\Lambda_i^2\frac{\partial w_i}{\partial\Lambda_i}(1-\Lambda_i^2)\sum_{k\in\mathcal{N}_i}(\Lambda_k - \Lambda_i)),\\ &= -c_1\mu\boldsymbol{\Lambda}^{\mathrm{T}}(PF(\underline{\mathcal{L}} + \underline{\mathcal{A}}) + (\underline{\mathcal{L}} + \underline{\mathcal{A}})^{\mathrm{T}}PF)\boldsymbol{\Lambda},\end{aligned} \tag{37}$$

where $F = W(\boldsymbol{\Lambda})\underline{W}(\boldsymbol{\Lambda}) - \frac{\partial W(\boldsymbol{\Lambda})}{2\partial\boldsymbol{\Lambda}}\underline{W}(\boldsymbol{\Lambda})\operatorname{diag}(\Lambda_2, ..., \Lambda_N)$. Thus, F is a diagonal matrix and $F = \operatorname{diag}(f_2, ..., f_N)$ with

$$f_i = w_i(1-\Lambda_i^2) + \frac{\partial w_i}{2\partial\Lambda_i}\Lambda_i(1-\Lambda_i^2). \tag{38}$$

Then, it follows from (35) that $f_i = 1$, $F = I_{N-1}$, and

$$\dot{V}(\boldsymbol{\Lambda}) = -c_1\mu\boldsymbol{\Lambda}^{\mathrm{T}}(P(\underline{\mathcal{L}} + \underline{\mathcal{A}}) + (\underline{\mathcal{L}} + \underline{\mathcal{A}})^{\mathrm{T}}P)\boldsymbol{\Lambda}. \tag{39}$$

By Assumption 2 and Lemma 2.3, $P(\underline{\mathcal{L}} + \underline{\mathcal{A}}) + (\underline{\mathcal{L}} + \underline{\mathcal{A}})^{\mathrm{T}}P$ is positive definite. Thus, $\boldsymbol{\Lambda}(t)$ converges to $\boldsymbol{0}_{N-1}$ as $t \to \infty$. Since $\gamma_1 = 0$, each $\gamma_i(t)$ converges to 0 as $t \to \infty$. Then, $\lim_{t\to\infty}\mathcal{L}(\boldsymbol{\theta}(t) - \boldsymbol{\alpha}) = \boldsymbol{0}_N$ by (30), and $\lim_{t\to\infty}\psi_{ki}(t) - \alpha'_{ki} = 0$, $i \in \mathcal{O}$, $k \in \mathcal{N}_i$. All these arguments are summarized in the following proposition.

Proposition 3.3: Consider $\|\mathcal{E}\|$ systems in the form of (8) and a sensor graph $\mathcal{G}$ under Assumption 2. If $[d_0^i\ \beta_0^i]^{\mathrm{T}} = [r\ \frac{\pi}{2}]^{\mathrm{T}}$, $i \in \mathcal{O}$, controllers (9) ensure that $\lim_{t\to\infty}\psi_{ki}(t) - \alpha'_{ki} = 0$, $i \in \mathcal{O}$, $k \in \mathcal{N}_i$, for any $\psi_{ki}(t_0) \in [0, 2\pi)$, i.e., Γ_2 is globally

asymptotically stable relative to Γ_1. ■

E. Proof of Theorem 3.1

Now, we are ready to prove Theorem 3.1 as follows.

Proof: Noting that $\Gamma_2 \subset \Gamma_1$, Propositions 3.2 and 3.3 indicate that condition (i) of Lemma 2.2 is satisfied under Assumptions 1–3. Proposition 3.2 also implies that $\boldsymbol{d}_0$ is uniformly bounded and thus condition (ii) of Lemma 2.2 is also satisfied. Since Γ_2 is compact, by Lemma 2.2, Γ_2 is globally asymptotically stable relative to Π under Assumptions 1–3. Theorem 3.1 is thus proved. ■

Remark 3.1: Assumption 1 implies that the proposed controller on the basis of the sensor graph $\bar{\mathcal{G}} = (\bar{\mathcal{O}}, \bar{\mathcal{E}})$ is distributed in the sense that the center is not known to all vehicles, i.e., $(0, i) \in \bar{\mathcal{E}}$ for some $i \in \mathcal{O}$. While in [6, 14, 16], the edges $(0, i)$ for each $i \in \mathcal{O}$ were assumed in $\bar{\mathcal{E}}$. In addition to Assumption 1, Assumption 3 is used to ensure the controlled vehicles can converge to the common circle around the center. Compared with [16] where direct distance measurements were also not required, the price for relaxing the assumption that $(0, i) \in \bar{\mathcal{E}}$ for each $i \in \mathcal{O}$, is that each vehicle needs to implemented the controller with the suggested methods by additionally measuring the relative heading angle to its neighbors or installing a onboard laser transmitter. Many existing works on circular formation control also require relative heading angle measurements [6, 7, 10–12, 15, 17], or absolute heading angle measurements [9, 14]. The relative heading angle measurements require each vehicle to be equipped with a camera and a visual marker for orientation. As shown in [27], each vehicle i can use the camera to detect the markers for orientation on its neighbors, and then the relative heading angles θ_k^i, $k \in \mathcal{N}_i$, can be directly measured. This process can be done along with measuring the bearing angles. Thus, the measurements of each vehicle only rely on a camera and visual markers mount on its neighbors, and does not need other sensors, such as radar and RF sensor, to measure distances. Alternatively, an Attitude and Heading Reference System (AHRS) used in [26] can be installed to provide heading angle measurements. It is noted that the obstruction of the line of sight is assumed to be negligible in this note. ■

Remark 3.2: Compared with [17], the result in this note has several advantages when r and ω_0 are known to all vehicles. First, the communication among vehicles and the memory of vehicles are not required. Second, direct distance measurements are not needed either. Finally, our result addresses the global convergence to any desired spaced formation instead of only an evenly-spaced one in [8, 16, 17]. Moreover, it is assumed in [17, 20] that graph $\bar{\mathcal{G}}'$ is a directed tree, which is a special case of graph $\bar{\mathcal{G}}'$ under Assumption 3. ■

Remark 3.3: Controller (10) reduces to (16) for vehicle i, $i \in \mathcal{O}$, if Assumption 1 reduces to the following assumption used in [6, 14, 16].

Assumption 4: $\bar{\mathcal{G}} = (\bar{\mathcal{O}}, \bar{\mathcal{E}})$ with $(0, i) \in \bar{\mathcal{E}}$, $\forall i \in \mathcal{O}$. ■

In this case, the "companion" vehicles are not needed, and relative heading angle measurements are not required. Thus, the requirement for local measurements becomes the same as that in [16]. Proposition 3.2 holds without Assumption 3, and controller consisting of (9) and (16) solves Problem 1 under Assumptions 2 and 4. Compared with [6, 14], direct distance measurements are not required, and any desired spaced formation can be achieved with only bearing angle measurements. ■

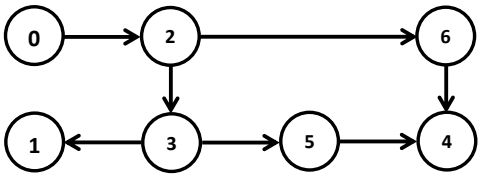

Fig. 2. The topology of the sensor graph $\bar{\mathcal{G}}$.

IV. An Illustrative Example

Consider a group of 6 nonholonomic vehicles in the form of (1). The sensor graph $\bar{\mathcal{G}}$ is given in Fig. 2 which satisfies Assumptions 1–3. The values of all variables in this example are in SI units and the units are omitted for convenience.

Velocity constraints (2) are given by $0.2 \leq v_i \leq 3$ and $-\pi \leq \omega_i \leq \pi$. The center is given by $\boldsymbol{p}_0 = [0\ 0]^{\mathrm{T}}$, and $[\omega_0\ r]^{\mathrm{T}}$ is set to $[1\ 1]^{\mathrm{T}}$. According to (11), the parameters μ, c_1 and c_2 are set to $\mu = 0.25$, $c_1 = \frac{3}{4}$, and $c_2 = \pi - \frac{7}{4}$ respectively. The initial states of vehicles are $\boldsymbol{p}_1(0) = [0\ 0]^{\mathrm{T}}$, $\boldsymbol{p}_2(0) = [3\ 1.5]^{\mathrm{T}}$, $\boldsymbol{p}_3(0) = [0.3\ 1.8]^{\mathrm{T}}$, $\boldsymbol{p}_4(0) = [2.4\ -1.6]^{\mathrm{T}}$, $\boldsymbol{p}_5(0) = [1.5\ -1.5]^{\mathrm{T}}$, $\boldsymbol{p}_6(0) = [-2.25\ -0.2]^{\mathrm{T}}$, $\theta_1(0) = -\frac{\pi}{2}$, $\theta_2(0) = \pi$, $\theta_3(0) = \frac{\pi}{3}$, $\theta_4(0) = -\pi$, $\theta_5(0) = \frac{5\pi}{6}$, and $\theta_6(0) = 0$.

Two circular formations with different spacing are studied. The first case considers an evenly-spaced formation along the semi-circle, described by $\boldsymbol{\alpha}_{\text{case 1}} = [0\ \frac{\pi}{6}\ \frac{\pi}{3}\ \frac{\pi}{2}\ \frac{2\pi}{3}\ \frac{5\pi}{6}]^{\mathrm{T}}$. The second case considers a spaced formation described by $\boldsymbol{\alpha}_{\text{case 2}} = [0\ \frac{\pi}{3}\ \frac{\pi}{2}\ \frac{7\pi}{6}\ \frac{11\pi}{6}\ \frac{4\pi}{3}]^{\mathrm{T}}$.

Fig. 3 presents the trajectories of all vehicles with controller (9)–(10) during 0–60s in both cases, which shows that the vehicles converge to the circular formation with desired spacing. Fig. 4 presents the distances $\|\boldsymbol{p}_i(t) - \boldsymbol{p}_0\|$ within 60s, which shows that the vehicles converge to the common circle with the given center $\boldsymbol{p}_0$ and radius r. Fig. 5 illustrates that the vehicles converge to the desired spaced formations. All these results verify effectiveness of the proposed controllers.

V. Conclusion

In this note, we have developed a distributed controller for nonholonomic vehicles of unicycle type, such that vehicles converge to a circular formation with desired spacing. The center is assumed to be known to only some vehicles. Each vehicle only needs to use local measurements from onboard senors, and direct distance measurements are not required. Our future work will focus on controller design for vehicles with disturbances and the obstruction of the line of sight, and analysis on collision avoidance.

Acknowledgment

The authors would like to thank the Associate Editor and all anonymous Reviewers for their valuable comments, and

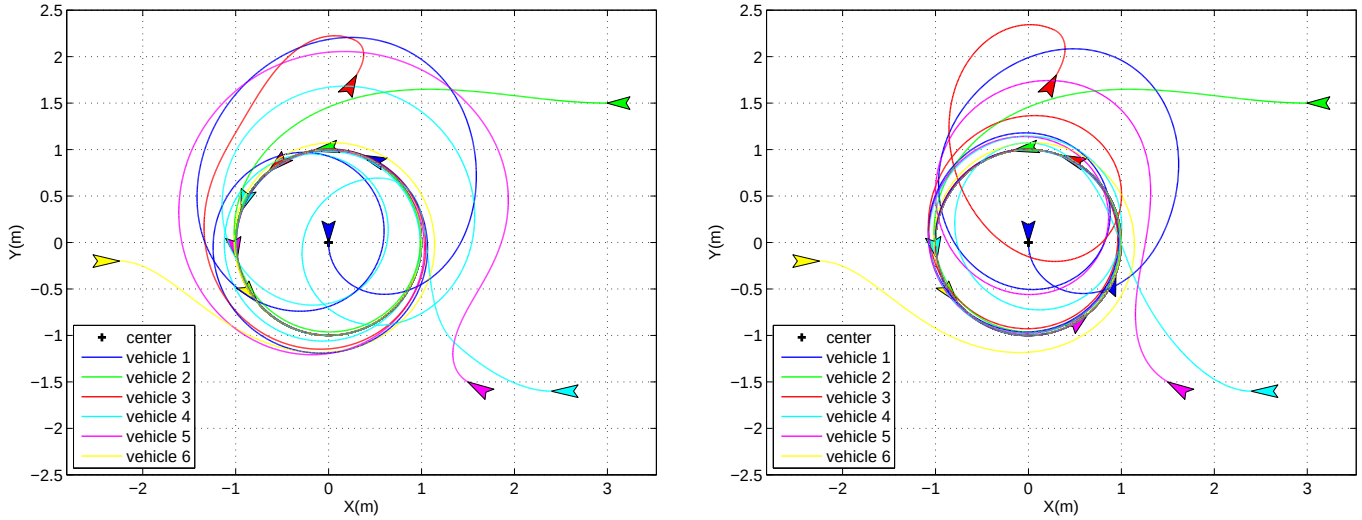

(a) Case 1 (b) Case 2

Fig. 3. Trajectories of all vehicles during 0-60s.

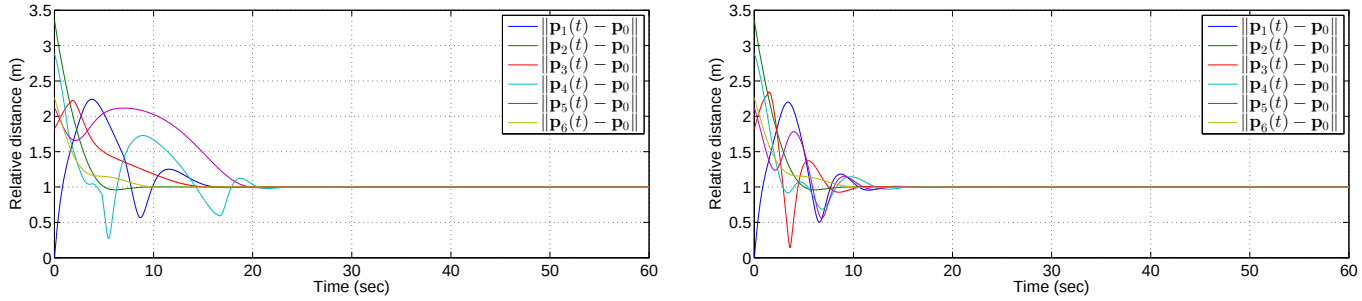

(a) Case 1 (b) Case 2

Fig. 4. Distance $\|\boldsymbol{p}_i(t)-\boldsymbol{p}_0\|$, $i=1,...,6$, during 0-60s.

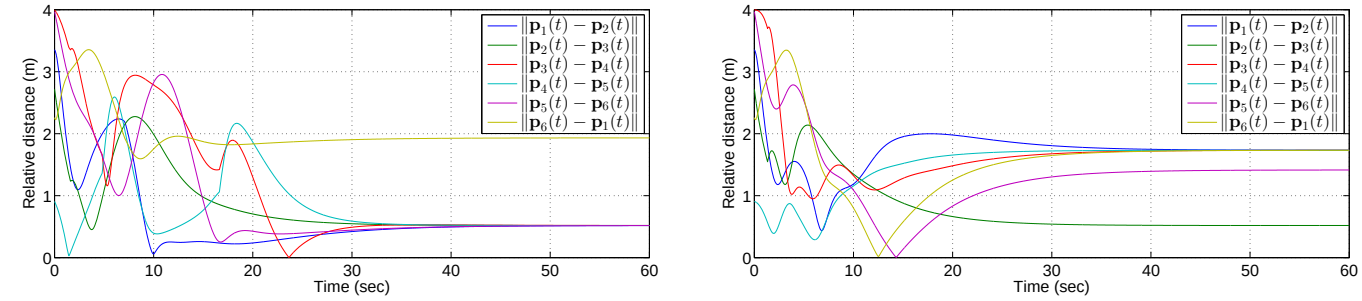

(a) Case 1 (b) Case 2

Fig. 5. Distance $\|\boldsymbol{p}_i(t)-\boldsymbol{p}_{(i+1)}(t)\|$, $i=1,..,5$, and $\|\boldsymbol{p}_6(t)-\boldsymbol{p}_1(t)\|$, during 0-60$s$.

Dr. Kai Wang at CUHK(Shenzhen) for his constructive dissuasions regarding the methods for controller implementation.

REFERENCES

[1] R. Olfati-Saber, J. A. Fax, and R. M. Murray, "Consensus and cooperation in networked multi-agent systems," *Proc. IEEE*, vol. 95, no. 1, pp. 215–233, 2007.

[2] Y. Cao, W. Yu, W. Ren, and G. Chen, "An overview of recent progress in the study of distributed multi-agent coordination," *IEEE Trans. Ind. Inf.*, vol. 9, no. 1, pp. 427–438, 2013.

[3] K.-K. Oh, M.-C. Park, and H.-S. Ahn, "A survey of multi-agent formation control," *Automatica*, vol. 53, pp. 424–440, 2015.

[4] J. A. Marshall, M. E. Broucke, and B. A. Francis, "Formations of vehicles in cyclic pursuit," *IEEE Trans. Autom. Control*, vol. 49, no. 11, pp. 1963–1974, 2004.

[5] J. A. Marshall, M. E. Broucke, and B. A. Francis, "Pursuit formations of unicycles," *Automatica*, vol. 42, no. 1, pp. 3–12, 2006.

[6] R. Sepulchre, D. A. Paley, and N. E. Leonard, "Stabilization of planar collective motion: All-to-all communication," *IEEE Trans. Autom. Control*, vol. 52, no. 5, pp. 811–824, 2007.

[7] R. Sepulchre, D. A. Paley, and N. E. Leonard, "Stabilization of planar collective motion with limited communication," *IEEE Trans. Autom. Control*, vol. 53, no. 3, pp. 706–719, 2008.

[8] N. Moshtagh, N. Michael, A. Jadbabaie, and K. Daniilidis, "Vision-based, distributed control laws for motion coordination of nonholonomic robots," *IEEE Trans. Rob.*, vol. 25, no. 4, pp. 851–860, 2009.

[9] Z. Chen and H.-T. Zhang, "No-beacon collective circular motion of jointly connected multi-agents," *Automatica*, vol. 47, no. 9, pp. 1929–1937, 2011.
[10] Z. Chen and H.-T. Zhang, "A remark on collective circular motion of heterogeneous multi-agents," *Automatica*, vol. 49, no. 5, pp. 1236–1241, 2013.
[11] M. I. El-Hawwary and M. Maggiore, "Distributed circular formation stabilization for dynamic unicycles," *IEEE Trans. Autom. Control*, vol. 58, no. 1, pp. 149–162, 2013.
[12] G. S. Seyboth, J. Wu, J. Qin, C. Yu, and F. Allgower, "Collective circular motion of unicycle type vehicles with non-identical constant velocities," *IEEE Trans. Control Network Syst.*, vol. 1, no. 2, pp. 167–176, 2014.
[13] N. Ceccarelli, M. Di Marco, A. Garulli, and A. Giannitrapani, "Collective circular motion of multi-vehicle systems," *Automatica*, vol. 44, no. 12, pp. 3025–3035, 2008.
[14] T. H. Summers, M. R. Akella, and M. J. Mears, "Coordinated standoff tracking of moving targets: control laws and information architectures," *J. Guid. Control Dynam.*, vol. 32, no. 1, pp. 56–69, 2009.
[15] Y. Lan, G. Yan, and Z. Lin, "Distributed control of cooperative target enclosing based on reachability and invariance analysis," *Syst. Control Lett.*, vol. 59, no. 7, pp. 381–389, 2010.
[16] R. Zheng, Y. Liu, and D. Sun, "Enclosing a target by nonholonomic mobile robots with bearing-only measurements," *Automatica*, vol. 53, pp. 400–407, 2015.
[17] X. Yu and L. Liu, "Distributed circular formation control of ring-networked nonholonomic vehicles," *Automatica*, vol. 68, pp. 92–99, 2016.
[18] R. Zheng, Z. Lin, M. Fu, and D. Sun, "Distributed control for uniform circumnavigation of ring-coupled unicycles," *Automatica*, vol. 53, pp. 23–29, 2015.
[19] X. Yu, L. Liu, and G. Feng, "Distributed circular formation control of multi-robot systems with directed communication topology," in *Proc. 35th Chin. Control Conf.*, Chengdu, China, 2016, pp. 8014–8019.
[20] Y. Dong and X. Hu, "Leader-following formation control problem of unicycles," in *Proc. 35th Chin. Control Conf.*, Chengdu, China, 2016, pp. 8154–8159.
[21] S. Zhao, F. Lin, K. Peng, B. M. Chen, and T. H. Lee, "Distributed control of angle-constrained cyclic formations using bearing-only measurements," *Syst. Control Lett.*, vol. 63, pp. 12–24, 2014.
[22] M. Deghat, I. Shames, B. D. Anderson, and C. Yu, "Localization and circumnavigation of a slowly moving target using bearing measurements," *IEEE Trans. Autom. Control*, vol. 59, no. 8, pp. 2182–2188, 2014.
[23] M. Deghat, L. Xia, B. Anderson, and Y. Hong, "Multi-target localization and circumnavigation by a single agent using bearing measurements," *Int. J. Robust Nonlinear Control*, vol. 25, no. 14, pp. 2362–2374, 2015.
[24] M. Basiri, A. N. Bishop, and P. Jensfelt, "Distributed control of triangular formations with angle-only constraints," *Syst. Control Lett.*, vol. 59, no. 2, pp. 147–154, 2010.
[25] A. N. Bishop, "A very relaxed control law for bearing-only triangular formation control," in *Proc. 18th IFAC World Cong.*, Milano, Italy, 2011, pp. 5991–5998.
[26] K. Wang, Y.-H. Liu, and L. Li, "Visual servoing trajectory tracking of nonholonomic mobile robots without direct position measurement," *IEEE Trans. Rob.*, vol. 30, no. 4, pp. 1026–1035, 2014.
[27] X. Liang, Y.-H. Liu, H. Wang, W. Chen, K. Xing, and T. Liu, "Leader-following formation tracking control of mobile robots without direct position measurements," *IEEE Trans. Autom. Control*, vol. 61, no. 12, pp. 4131–4137, 2016.
[28] W. Ren and R. W. Beard, "Trajectory tracking for unmanned air vehicles with velocity and heading rate constraints," *IEEE Trans. Control Syst. Technol.*, vol. 12, no. 5, pp. 706–716, 2004.
[29] K. S. Narendra and A. M. Annaswamy, "Persistent excitation in adaptive systems," *Int. J. Control*, vol. 45, no. 1, pp. 127–160, 1987.
[30] M. I. El-Hawwary and M. Maggiore, "Reduction theorems for stability of closed sets with application to backstepping control design," *Automatica*, vol. 49, no. 1, pp. 214–222, 2013.
[31] H. Zhang, Z. Li, Z. Qu, and F. L. Lewis, "On constructing lyapunov functions for multi-agent systems," *Automatica*, vol. 58, pp. 39–42, 2015.
[32] J. Guo, G. Yan, and Z. Lin, "Local control strategy for moving-target-enclosing under dynamically changing network topology," *Syst. Control Lett.*, vol. 59, no. 10, pp. 654–661, 2010.
[33] H. K. Khalil, *Nonlinear Systems, (3rd edn)*. PrenticeHall: Upper Saddle River, NJ, 2002.
[34] W. Ren and R. W. Beard, "Consensus seeking in multiagent systems under dynamically changing interaction topologies," *IEEE Trans. Autom. Control*, vol. 50, no. 5, pp. 655–661, 2005.